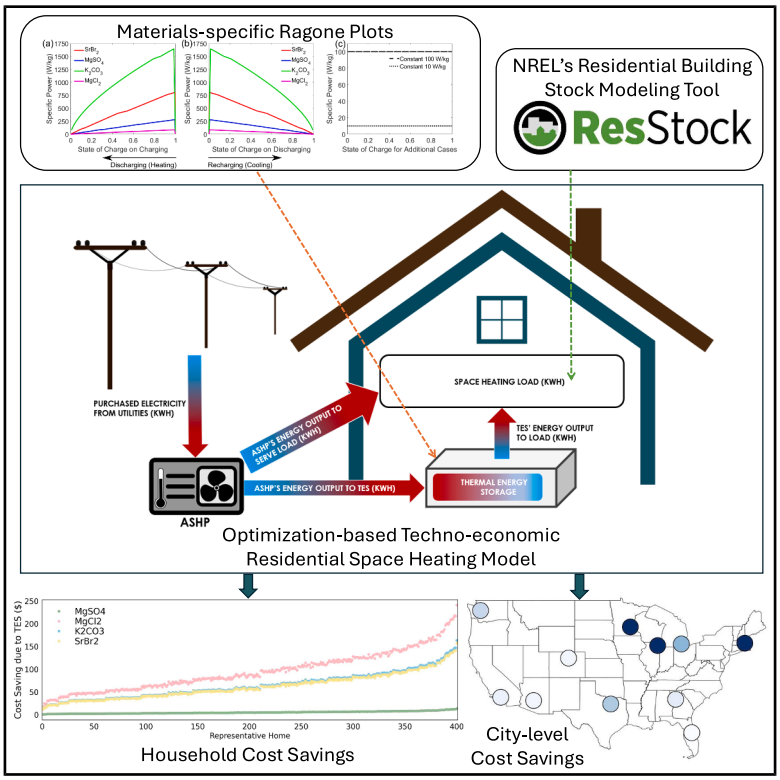
Cell Reports
Sustainability

Article

Assessing the value of coupling thermal energy storage with air source heat pumps for residential space heating in US cities

Graphical abstract



Authors

An T. Pham, Bryan Kinzer, Ritvik Jain, Rohini Bala Chandran, Michael T. Craig

Correspondence

anph@umich.edu

In brief

Pham et al. examine the value of salt hydrate thermal energy storage in reducing heating costs in US households when dispatched with air source heat pumps. This study emphasizes the drivers of the magnitude of cost savings, including salt materials, heating load profiles, designs of the thermal energy storage systems, and the climates they operate in. It also identifies the salt attributes that would make salt hydrate TES more economically effective, yielding important insights for researchers, TES developers, and policymakers.

Highlights

- We quantify the space heating value of salt hydrate TES coupled with ASHPs in US cities
- Salt hydrate TES can reduce household heating costs by 44% in cold climates
- Cost savings from salt hydrate TES vary widely between households, salts, and climates
- $SrBr_2$-based TES can exceed the US Department of Energy's $15/kWh TES cost target

Pham et al., 2025, Cell Reports Sustainability 2, 100460
September 26, 2025 © 2025 The Author(s). Published by Elsevier Inc.
https://doi.org/10.1016/j.crsus.2025.100460

CellPress

Cell Reports Sustainability

CellPress
OPEN ACCESS

Article

Assessing the value of coupling thermal energy storage with air source heat pumps for residential space heating in US cities

An T. Pham,[1,4,*] Bryan Kinzer,[2] Ritvik Jain,[1] Rohini Bala Chandran,[2] and Michael T. Craig[1,3]
[1]School for Environment and Sustainability, University of Michigan, 440 Church St, Ann Arbor, MI 48109, USA
[2]Department of Mechanical Engineering, University of Michigan, 2350 Hayward St, Ann Arbor, MI 48109, USA
[3]Department of Industrial and Operations Engineering, University of Michigan, 1891 IOE Building 1205, Beal Ave, Ann Arbor, MI 48109, USA
[4]Lead contact
*Correspondence: anph@umich.edu
https://doi.org/10.1016/j.crsus.2025.100460

SCIENCE FOR SOCIETY Thermal energy storage (TES) can help address the challenges that widespread adoption of air source heat pumps (ASHPs) are facing, including improving heat pumps' efficiencies during cold periods. In this study, we quantify the cost saving and load shifting values of thermochemical salt hydrate TES coupled with ASHP for residential space heating application across US cities in different climates. Our findings show that salt hydrate TES can effectively reduce residential space heating costs when coupled with ASHP, particularly in cold-climate cities. For example, in Boston, Minneapolis, and New York City, we find that salt hydrate TES can save between 10% and 44% of annual household heating costs. Annual cost savings from salt hydrate TES vary widely, depending on households' heating load profiles, the types of salts used as materials, TES designs and sizing methods, and climates. Additionally, we identify the most promising salt material in this study, $SrBr_2$, which can reach and exceed US Department of Energy's TES cost target in most cold-climate cities. This research yields several important insights for salt hydrate TES research and development. We highlight the attributes of salt hydrates that would make them more economically effective, as well as emphasize the potential market of commercially produced salt hydrate TES to provide energy input for residential space heating demand and the potentially large role salt hydrate TES could play in decarbonizing the residential sector.

SUMMARY

Widespread air source heat pump (ASHP) adoption faces several challenges that thermochemical salt hydrate energy storage can mitigate. We quantify the space heating value of four salts—$MgSO_4$, $MgCl_2$, K_2CO_3, and $SrBr_2$—coupled with ASHPs across 4,800 households in 12 US cities by embedding salt-hydrate-specific Ragone plots into a techno-economic model of coupled ASHP-thermal energy storage (TES) operations. In Detroit, salt hydrate TES can reduce household annual electricity costs by 5%–8%. Cost savings from TES vary widely between households, salts, and climates. We identify the most promising salt in this study, $SrBr_2$, due to its high energy density and low humidification parasitic load. Breakeven capital costs of $SrBr_2$-based TES can reach $17/kWh, making it the only salt studied to reach and exceed the US Department of Energy's $15/kWh TES cost target. Sensitivities highlight the importance of variable TES sizing and efficiency losses in the value of TES.

INTRODUCTION

Decarbonizing the residential sector hinges on decarbonizing residential space heating (RSH). In the US, over 21% of primary energy consumption in 2021 was in the residential sector,[1] 32% of which was consumed for space heating.[2] A key decarbonization strategy for residential heating is replacing fossil-based heating with air source heat pumps (ASHPs).[3–5] However, widespread residential ASHP adoption faces several challenges, including poor efficiencies (or coefficients of performance [COPs]) in extreme cold despite cold-weather design improvements,[6] high capital costs, and long payback periods.[7] Widespread ASHP adoption might also increase peak electricity demand, especially in winter peaking power systems,[8,9]

This is an open access article under the CC BY-NC-ND license (http://creativecommons.org/licenses/by-nc-nd/4.0/).

which must be accounted for in power system planning and operation.

Various energy storage technologies, including lithium-ion batteries, flow batteries, and thermal energy storage (TES) (including ice storage), can be coupled with ASHPs in residential heating. Here, we perform the first broad assessment of a technology that might mitigate each of these challenges: salt hydrate TES. On-site short-term TES is particularly promising for coupling with ASHP.[5,10–17] Odukomaiya et al.[12] shows that in a wide range of scenarios, TES can be more cost effective than battery storage when coupled with ASHP. TES can use diverse materials as heating or cooling sources. Water tank heat storage, for instance, is widely used for building heating.[18,19] However, it has low energy density and unstable range of working temperatures,[19] which are the challenges that phase change materials (PCMs) with large latent heat enthalpy can overcome. Many types of PCMs exist, including ice storage, paraffins, alcohols, and salt hydrates.[19–21] Our analysis focuses on salt hydrates, an immature but promising TES option. Salt hydrates face several challenges for TES applications, such as supercooling, phase separation, and material corrosion compared with organic PCMs. However, they have several advantages relative to other TES options, including high energy densities (2–10 times higher than sensible heat capacity of water[22–24] and organic PCMs[20]), lower losses than other residential TES materials,[23,25–29] reasonable stability, and low toxicity.

In salt hydrate TES, heat is generated during salt hydration (i.e., when it uptakes water) and consumed during salt dehydration (i.e., when it releases water). During hydration, water (vapor) is impregnated into the salt lattice structure.[30] Despite their promise, salt hydrate TES has yet to be commercialized; rather, most existing work examines prototype salt hydrate TES devices.[31] Furthermore, many potential salt hydrates might not be cost effective due to high material and/or device costs.[30,31]

The cost effectiveness of TES in a coupled TES-ASHP system depends on multiple factors, including TES materials and designs, ASHP designs, the local climate, and buildings' heating load profiles. In the TES-heat pump system literature, techno-economic studies quantify the cost effectiveness of different TES-heat pump systems in realistically scaled building heating and cooling applications in diverse global geographical locations.[5,10,32–39] However, these analyses are limited to small samples of buildings (typically one or two buildings in a single city or location) and narrow time windows in several cases (e.g., one or two representative day(s) in a season). Conclusions from these studies are mixed, as some find significant potential in cost saving and peak load reduction from coupling TES with heat pumps,[10,38,39] while another finds TES is not cost effective.[36] Most importantly, only one recent study[40] considers high energy density salt hydrate TES. This study specifically analyzes the techno-economic performance of one type of salt hydrate ($SrCl_2$) in four prototypical buildings in each of four US cities.[40] The main conclusion of this study is that salt hydrates' energy density can be improved when operating in humid climates, resulting in higher efficiency of the buildings' heating, ventilation, and air conditioning (HVAC)-TES systems. This study, although equally important, focuses more on the design and integration of salt hydrate TES system, which differs from our approach in that in the latter we compare operational cost savings from load shifting calculations based on reasonable kinetic data for various salts. Additionally, this study, similar to the prior ones, analyzes a limited number of buildings, missing significant heterogeneity in the US building stock, analyzes only one high energy density salt hydrate, and yields no techno-economic guidance for salt hydrate TES development in residential applications.

In this study, we conduct a techno-economic assessment of salt hydrate TES in RSH application. To model realistic operation of salt hydrate TES, we use Ragone plots, which indicate the relationship between energy and power density given material properties, and expected influences of device designs and operating conditions.[30] Ragone plots have been used in a wide range of applications, most notably for batteries to guide storage device designs.[41] While the application of Ragone plots for TES devices is an emerging research topic,[42–44] it has been used in techno-economic analyses of stand-alone battery storage.[45,46] Thus far techno-economic analyses have not been specifically applied to salt-based TES and preclude the incorporation of Ragone plots. To overcome these knowledge gaps, this study applies the Ragone framework, first developed and experimentally validated by Kinzer et al.[30] for select salt hydrates, including a $SrBr_2$ vermiculite, to project cost savings for salt-based TES systems.

We quantify the value of coupling salt hydrate TES with ASHP across 4,800 representative households spread across 12 US cities. We specifically quantify the value of four salt hydrates—$MgSO_4$, $MgCl_2$, K_2CO_3, and $SrBr_2$—with varying power and energy densities and of six TES designs with varying charging and discharging limits and storage sizes (salt masses). We quantify TES value in terms of residential heating electricity cost savings and peak electricity consumption reduction. In so doing, we make two key contributions. First, we quantify the value of diverse TES materials and designs when coupled with ASHPs across a broad set of US households, providing unique guidance for salt hydrate TES materials and device development. Next, we incorporate salt-hydrate-specific Ragone plots, developed first by Kinzer et al.,[30] into a techno-economic analysis framework, advancing modeling capabilities to assess cost effectiveness of TES in residential applications. The purpose of our analysis is to generate a first-order estimate of economic viability of salt hydrate TES for space heating by analyzing its value across a large number of US households. To achieve this desired scale, our analytical approach explicitly models key elements of TES-ASHP design and operation and implicitly models other such elements (eliding some system design and operational details) using simple parameterizations. Due to uncertainty in capital costs of the emerging TES technologies considered in this study, we choose to minimize total operating costs, then we use estimated operational savings to estimate breakeven capital costs. Our breakeven capital costs reflect the maximum cost a household could spend on a TES device while still achieving net savings from a TES device, thereby providing cost benchmarks for TES developers to reach.

We develop an optimization-based techno-economic model of meeting RSH demand with an ASHP coupled with a salt hydrate TES device (hereafter referred to as the RSH, model). In

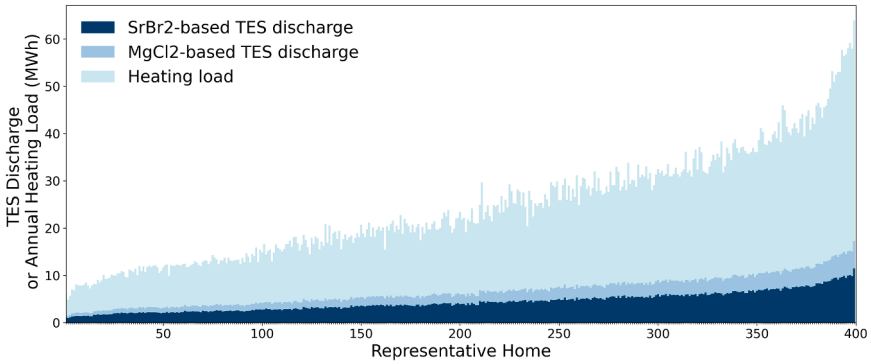


Figure 1. $MgCl_2$- and $SrBr_2$-based TES energy outputs across 400 representative Detroit homes in 2018

Homes are sorted from lowest to highest peak heating load. The heights of the azure, light blue, and dark blue color bars indicate heating loads, $MgCl_2$-based TES discharges, and $SrBr_2$-based TES discharges across homes, respectively.

the coupled TES-ASHP system, the TES and ASHP can serve heating demand, and the ASHP can charge the TES. We model an open-cycle ASHP-TES system. When discharging, recirculating indoor air is humidified if needed and passed through the TES device, and when charging, warm air from the ASHP is passed through the TES device (see section TES materials and designs for more TES system details). We embed TES material-specific Ragone plots into the RSH model using a piecewise linear approximation.

For each studied residential home, the RSH model minimizes space heating costs or peak demand by deciding ASHP capacity and/or ASHP and TES operations. Using the RSH model, we quantify two key values of salt hydrate TES: (1) cost savings from avoided electricity purchases for space heating and (2) reductions in peak electricity demand for space heating. We run the RSH model for 4,800 representative single detached homes in 12 climatically diverse US cities, or 400 representative homes in each US city, on an hourly basis for 2018 weather. This home sample size represents variability in housing characteristics within the total building stock in each city.[47] For each studied residential home, we run the RSH model in two steps for computational tractability. In the first step, the model optimizes the home's ASHP's capacity based on the home's annual peak heating demand. In the second step, using the optimized ASHP capacity from the first step as a parameter input, the model optimizes hourly operations of the TES and ASHP, which determine electricity purchases. In this step, to quantify the value of TES, we run the RSH model for each household twice, once with only an ASHP and once with a coupled ASHP-TES system. Key RSH model inputs include hourly heating demands, hourly ASHP COPs (driven by ambient temperatures), residential electricity retail prices, and TES Ragone plots and efficiency. Given uncertainties in future TES designs, we quantify the sensitivity of our results to TES sizes and designs.

RESULTS

ASHP and TES operations across TES materials in a cold-climate city

We first present detailed results for Detroit, a cold-climate city, for our four salt hydrates—$MgSO_4$, $MgCl_2$, K_2CO_3, and $SrBr_2$—to build intuition for their operation, sizing, and economics, then scale our results to 12 US cities. All reported energy (kWh) values refer to electric energy (kWhe). Across the four salts considered, there are clear patterns of TES operations (Figure S11). In general, TES discharges when ASHP's COP declines and/or is at a local minimum and charges when ASHP's COP rises and/or is at a local maximum. While this operational relationship applies to all studied TES materials, TES discharging and charging differ between salts due to their different power and energy densities and the relationships between their power and energy densities (Figure S12B). Salts that have relatively higher energy densities compared with their power densities such as $MgCl_2$ can discharge and charge for larger magnitudes and for longer periods of time and can engage in more cycles per day than relatively lower energy density salts such as $SrBr_2$.

Figure 1 compares annual TES discharge as a fraction of annual heating load across our 400 Detroit residential single family detached homes (hereafter "residential homes" or just "homes") when a relatively high energy density salt ($MgCl_2$) and a relatively lower energy density salt ($SrBr_2$) are used as TES materials. Across individual homes, loads shifted by TES differ widely. $MgCl_2$ shifts between 1.2 and 17.2 MWh (26%–27%) of annual heating load, while $SrBr_2$ shifts between to 0.8 and 11.5 MWh (17%–18%) of annual heating load. Aggregating across 400 representative homes, TES can shift up to 2.6 GWh (27%) of total annual space heating load when coupled with ASHP. Specifically, $MgSO_4$-, $MgCl_2$-, K_2CO_3-, and $SrBr_2$-based TES, respectively, shifts 0.15 GWh (1.5%), 2.6 GWh (27%), 1.8 GWh (19%), and 1.7 GWh (18%) of total annual space heating load (Figure S10). Each of these 400 Detroit homes represents 664 actual homes (Table S5); therefore, city-wide, $MgSO_4$-, $MgCl_2$-, K_2CO_3-, and $SrBr_2$-based TES can respectively shift 0.1, 1.7, 1.2, and 1.1 TWh of the city's total annual space heating load, respectively.

Salt hydrates that have relatively higher energy density (and thus higher energy capacity) ($MgCl_2$, see Table 1) have the potential to shift more load within and across homes (Figures S10A and S10B) than salts with relatively higher power density but lower energy density (and thus limited energy capacity) (K_2CO_3 and $SrBr_2$) (Figures S10C and S10D). While $MgSO_4$ has a relatively higher energy density, it also has a large parasitic load due to humidification requirements, reducing its load shifting utilization.

Economic value of TES for RSH in a cold-climate city

To quantify the economic value of coupling TES with ASHP in meeting RSH demand, we calculate total annual costs of purchasing electricity for each home for two heating systems: (1) ASHP only and (2) a coupled TES-ASHP system. In Detroit, a cold-climate city, the total annual cost of meeting space heating

Table 1. Power and energy requirements for the four salts used as TES materials in our study

Salt	Reaction enthalpy (kWh/kg)	Specific power at peak load (kW/kg)	Data source
$MgSO_4$	0.750	0.281	Linnow et al.[48]
$MgCl_2$	0.193	0.085	Hawwash et al.[49]
K_2CO_3	0.186	1.646	Gaeini et al.[50]
$SrBr_2$	0.356	0.811	Cammarata et al.[22]

demands for 400 representative homes with only ASHP is $602,000. Since each representative home represents 664 actual Detroit homes in ResStock[47] (Table S5), the total annual cost of meeting space heating demands with ASHP for all single detached family homes in Detroit is $400 million.

Relative to the only ASHP system, coupling TES with ASHP yields annual heating cost savings across 400 representative Detroit homes of $2,012 (0.3%), $38,009 (6.3%), $25,764 (4.3%), and $24,746 (4.1%) for $MgSO_4$-, $MgCl_2$-, K_2CO_3-, and $SrBr_2$-based TES, respectively. These are equivalent to annual cost savings across all actual Detroit homes of $1.3, $25.2, $17.1, and $16.4 million for $MgSO_4$, $MgCl_2$, K_2CO_3, and $SrBr_2$-based TES, respectively. Between homes, annual cost savings from TES differ widely, from $0.7 to $14 (0.2%–0.4%) with average of $5 and standard deviation of $3 to $18–$241 (5.4%–7.6%) with average of $95 and standard deviation of $43 and $13–$164 (3.6%–5.2%) with average of $64 and standard deviation of $29 and $12–$157 (3.5%–5.0%) with average of $62 and standard deviation of $28 if $MgSO_4$, $MgCl_2$, K_2CO_3, and $SrBr_2$ are TES materials, respectively (Figure 2). These wide differences in cost saving across homes reflect the homes' wide range of heating loads, with higher heating load homes having higher TES discharging and cost savings.

The cost effectiveness of each TES salt depends the size of salt mass needed for TES operation. We model the size of each of the salt hydrates used as TES materials in kg. Here, we size TES using variable sizing, in which the TES salt mass is sized based on peak heating load of each building. Details on how we size TES are in the supplemental information. We also consider incremental sizing and fixed sizing methods, which we include in sensitivity analysis.

To compare the cost effectiveness among TES salts, we also quantify the annual cost savings from TES per kg of salt. $SrBr_2$ is the most cost-effective salt, saving $1.8/kg to $2.4/kg per year across our 400 Detroit homes, or $2.2/kg on average per year. $SrBr_2$ is followed by K_2CO_3, which saves between $1.0/kg and $1.3/kg ($1.2/kg on average) per year; then $MgCl_2$, which saves between $0.7/kg and $0.9/kg ($0.8/kg on average); and finally $MgSO_4$, yielding cost saving between $0.08/kg and $0.15/kg ($0.13/kg on average). Cost effectiveness (or annual cost saving per kg) of each salt depends on the operation of each TES salt, which in turn depends on their energy density and parasitic load. $MgSO_4$ has low cost effectiveness due to its significant humidification parasitic load, while K_2CO_3 and $MgCl_2$ have lower energy density (K_2CO_3) or lower energy and power density ($MgCl_2$) than $SrBr_2$, limiting the amount and duration of their discharge.

Future salt hydrate TES capital and installation costs are highly uncertain. Using the cost savings from TES calculated above, we calculate a breakeven cost per MWh for each TES at each household. These breakeven costs reflect the maximum cost a household could spend on a TES device while still achieving net savings from a TES device. Assuming a targeted TES device lifetime of 20 years,[51] the breakeven costs of $MgSO_4$-, $MgCl_2$-, K_2CO_3-, and $SrBr_2$-based TES across 400 representative Detroit homes are on average $2.7, $16, $24, and $43 per kg, respectively (Figure S14). We calculate these breakeven costs as the average across households of total 20-year TES cost savings (or 20 times annual cost savings quantified above) divided by the TES salt mass. Due to different enthalpies among salts, these $/kg breakeven costs are, on average, equivalent to breakeven costs of $2.0/kWh, $3.1/kWh, $4.4/kWh, and $15.4/kWh thermal for $MgSO_4$-, $MgCl_2$-, K_2CO_3-, and $SrBr_2$-based TES, respectively (Figure 3). Between homes, the breakeven costs of $MgSO_4$-, $MgCl_2$-, K_2CO_3-, and $SrBr_2$-based TES vary from $1.2 to $2.4, $2.5 to $3.3, $3.6 to $4.8, and $12.7 to $16.7 per kWh thermal, respectively. Differences in breakeven costs between salts exceed differences in breakeven costs between households.

Load shifting and economic value of TES across US cities

We run our RSH model for 400 representative homes and the most promising salt identified above ($SrBr_2$) in each of 12 cities that span three climates —cold (Boston, Boulder, Chicago, Detroit, Minneapolis, and New York), mild (Atlanta and Seattle), and hot (Dallas, Los Angeles, Orlando, and Phoenix).[52] Summing across these representative homes by city, $SrBr_2$-based TES operation shifts from 0.04 to 11.6 TWh (20% to 38%) of total annual heating loads (Figure 5D) and incidentally reduces annual peak heating loads between 10.7% and 22.5% (16 MWh–4.1 GWh) (Figure 5C). Using TES to maximize peak load shifting rather than minimizing household costs could increase peak load reduction from 2% to almost 12% in a cold-climate city (supplemental information; Figure S13). Load shifting by TES saves up to $699 (19%) of total space heating costs annually in an individual home across cold-climate cities, $208 (12%) annually in an individual home in mild climate cities, and $77 (15%) annually in an individual home in hot climate cities (Figure 4A).

Cities in colder climates in general can save more with TES because they have higher heating load and more hours in which their ASHPs become inefficient. As a result, breakeven costs of $SrBr_2$-based TES in cold-climate cities are much higher than those in mild and hot climate cities (Figure 4B). Breakeven costs are highest in Minneapolis at $29–$45/kWh thermal across households, followed by in New York City at $17–$39/kWh thermal and Boston at $18–$27/kWh thermal. In mild climate cities, Seattle has the highest breakeven costs for TES at $8–$14/kWh thermal across households. In hot climate cities, Dallas has the highest breakeven costs for TES at $3–$9/kWh thermal across households.

Scaling our results to city-wide level, Figure 5 illustrates annual cost savings, breakeven costs, and peak heating load reduction and total load shifting due to $SrBr_2$-based TES across 12 cities. Annual city-wide cost savings reach up to $602 million in New York City (omitted from Figure 5A as it is an outlier) but other

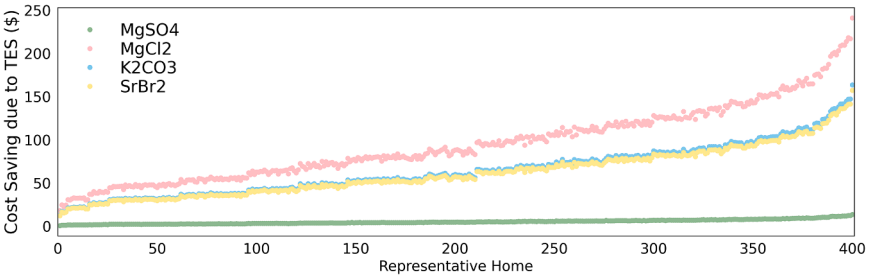


Figure 2. Annual cost savings in 400 representative Detroit homes from coupling TES of different salt hydrates with ASHP

Homes are sorted in order of lowest peak load to highest peak load.

11 cities have total annual cost savings between to $0.11 to $37 million (Figure 5A). Cost savings differ widely across cities. In a cold-climate city except New York City, annual cost saving due to TES ranges from $1.8 million (7%) (Boulder) to $37 million (10%) (Boston). Average breakeven costs for $SrBr_2$-based TES in a cold-climate city can reach $39/kWh thermal, but they are at most $12/kWh thermal in mild and $6/kWh thermal in hot climate cities (Figure 5B). These results emphasize the potential cost effectiveness of TES in cold-climate homes.

Sensitivity analysis

We test the robustness of our results for either all salt hydrates or just $SrBr_2$ to alternative TES and ASHP design and operational schemes in a cold-climate city (Detroit) (Table 3). One sensitivity modestly increases the value and cost effectiveness of TES; all others modestly or significantly reduce its value and cost effectiveness. For all four salt hydrates, increasing non-parasitic losses from 2% to 5% and from 2% to 10% would respectively reduce annual cost savings by between 3% and 11% and between 13% and 25% across households and salt hydrates (Table S10; section TES materials and designs). Alternative TES operational schemes could require greater humidification needs, resulting in parasitic losses of 44% to 70% across salt hydrates (compared with our base case where only $MgSO_4$ has humidification-driven losses of 39%) (Table SI.10; section TES materials and designs). At these parasitic losses in Detroit, TES cost savings decrease by 39%–93% across households and salt hydrates, and breakeven costs decrease by 9% to 82%. $SrBr_2$ remains the salt hydrate with the greatest breakeven costs for households, with breakeven costs of above $10/kWh thermal even under 44% parasitic loss and additional non-parasitic losses. Finite rather than variable TES sizing, which might occur if TES is commercialized, would reduce TES breakeven capital costs by 9%–42% due to oversizing across salts despite increasing annual household cost savings by 23%–71%. Using a gas furnace rather than electric baseboard as the ASHP backup would reduce $SrBr_2$ cost savings by roughly 19%–24% across homes and lead to up to 20% lower breakeven costs. Finally, running TES at a constant specific power output[53] (rather than variable output based on a Ragone plot) would increase breakeven costs of $SrBr_2$ by 3%. For more details, see the supplemental information.

DISCUSSION

To guide salt hydrate TES research and development, we provided the first broad techno-economic analysis of salt hydrate TES in RSH applications using Ragone plots for four TES materials[30] and heating profiles for 4,800 households across 12 US cities. We found that salt hydrate TES can effectively reduce RSH costs when coupled with ASHP, particularly in cold-climate cities. In Boston, Minneapolis, and New York City, for instance, we found that salt hydrate TES could save 10%–44% of household heating costs. Given these savings, we found households in Detroit could pay up to $2.7, $16, $24, and $43 per kg (or $1.0, $5.7, $8.5, and $15.3 per kWh thermal output) for $MgSO_4$, $MgCl_2$, K_2CO_3, and $SrBr_2$ salt, respectively, in a salt hydrate TES device and still break even, i.e., save money. $SrBr_2$ yields the highest cost saving per kg among the four salts due to its relatively high reaction enthalpy and power rating, and low parasitic humidification needs at typical residential indoor temperature, driving high energy output from a relatively small volume of salt. Assuming 20-year lifetime of the TES device, our breakeven costs capture the total system cost for the TES device to be cost effective, which includes installation cost, cost of initial purchase and replacement of the salt, and capital costs of the TES device components such as heat exchanger, storage tank, and condenser. Our breakeven costs provide upper bounds, or research and development (R&D) targets, for total TES device costs for economic viability in RSH. The other lower energy density salts' breakeven costs fall far below that of $SrBr_2$, which means much higher cost reductions would be needed for

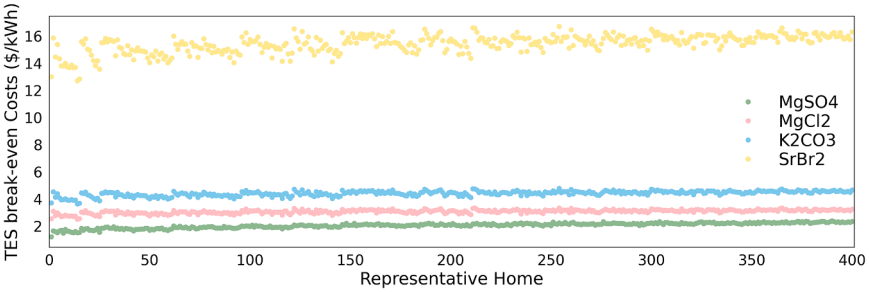


Figure 3. Breakeven costs in 400 representative Detroit homes from coupling TES of different salt hydrates with ASHP

Homes are sorted in order of lowest peak load to highest peak load.

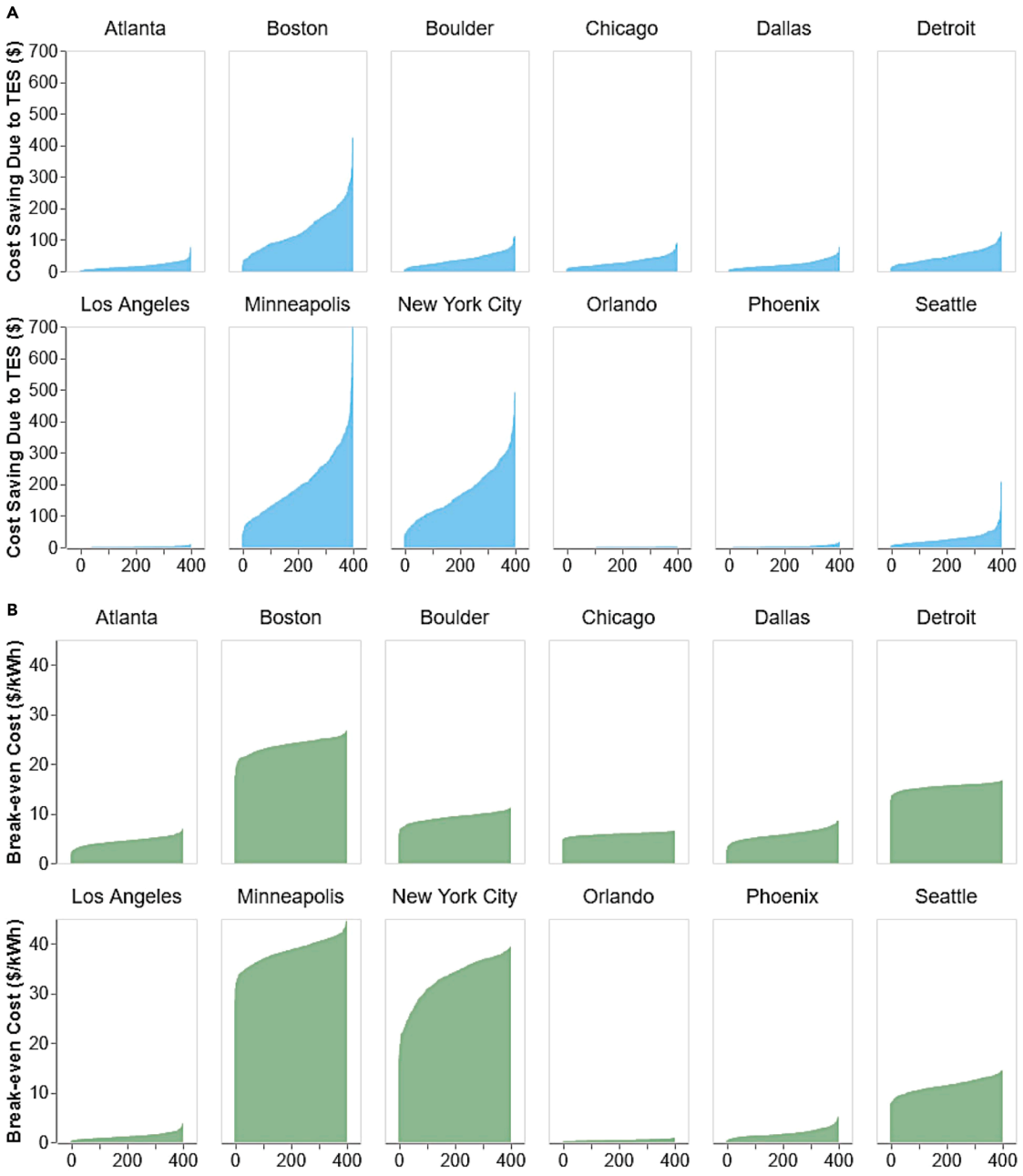


Figure 4. Cost savings and breakeven costs of $SrBr_2$-based TES in 400 representative homes in 12 US cities

Cost savings and breakeven costs in each city are sorted in order from lowest to highest. TES sizes here are determined using variable sizing method which depends on each home's peak load.

(A) Cost savings in $ due to $SrBr_2$-based TES in 400 representative homes in 12 US cities.

(B) Breakeven costs in $/kWh of $SrBr_2$-based TES in 400 representative homes in 12 US cities.

them to be cost effective in RSH applications. Our household-level results also provide an estimate of the size the market potential for TES in RSH. In cold climates, for instance, $SrBr_2$-based TES breakeven costs exceed $10/kWh in most homes in Boston, Boulder, Detroit, Minneapolis, and New York City, but in no homes in Chicago. In mild and hot climates, salt hydrate TES is less cost effective due to lower heating needs and more efficient ASHP operations. In these climates, except for Seattle, $SrBr_2$-based TES could only reach breakeven costs of less than $6/kWh thermal.

Through a wide range of sensitivity analysis, we emphasized the importance of TES sizing methods and designs that developers of future TES devices should consider. First, strategically sizing TES based on household energy needs significantly

CellPress
OPEN ACCESS

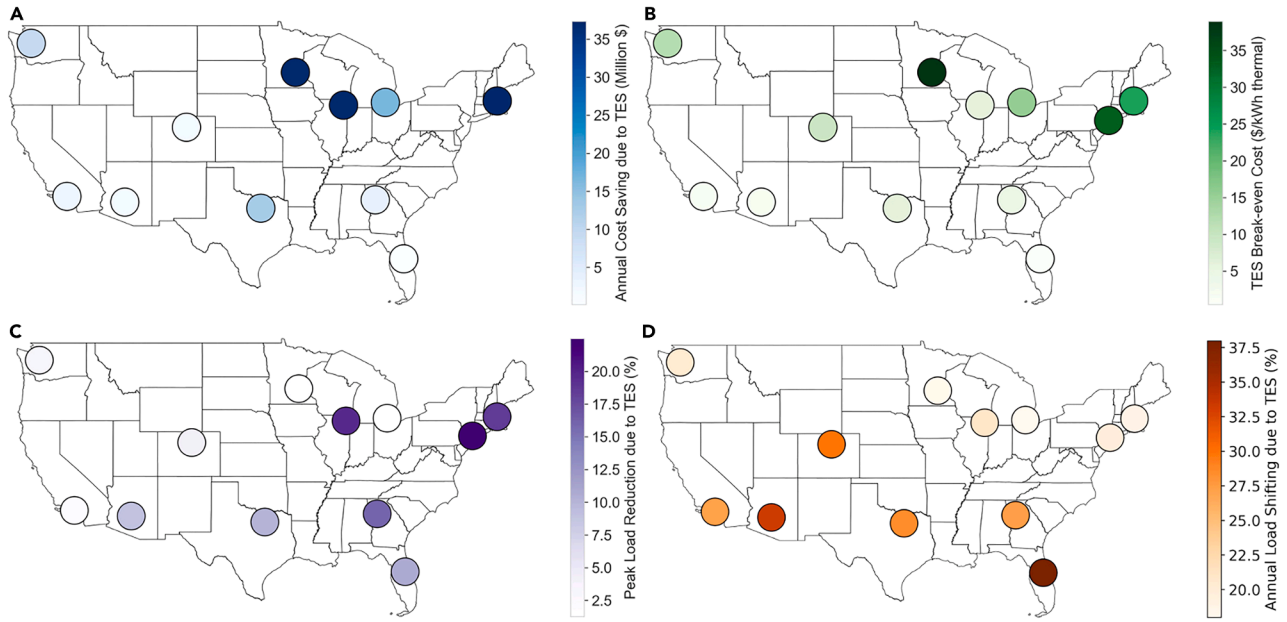


Figure 5. Economic and load shifting values of $SrBr_2$-based TES across 12 US cities

Annual cost savings ($) (A) and average breakeven costs ($/kWh thermal) (B) in 12 US cities due to $SrBr_2$-based TES. Total annual amount of peak load reduction (%) (C) and total annual amount of load being shifted (%) (D) due to $SrBr_2$-based TES. New York City is omitted from (A) due to being an outlier. TES sizes here are determined using variable sizing method which depends on each building's peak load.

TES sizes here are determined using variable sizing method which depends on each home's peak load.

(A) Annual cost savings (million $) due to $SrBr_2$-based TES in 12 US cities.

(B) $SrBr_2$-based TES breakeven costs ($/kWh thermal) in 12 US cities.

(C) Peak load reductions (%) due to $SrBr_2$-based TES in 12 US cities.

(D) Annual load shifting (%) due to $SrBr_2$-based TES in 12 US cities.

increases the value of TES rather than using predetermined TES sizes, which can lead to under- or oversizing of TES. Second, homes with electric baseboard backup, which is the most common ASHP backup system, benefit more from TES than homes with gas furnaces backup. Finally, consistent with N'Tsoukpoe and Kuznik,[31] our results across all salts show that choosing TES materials with low humidification parasitic load is key in raising the cost effectiveness of TES-ASHP systems. Government support for research and development should therefore target development of salt hydrates with low humidification parasitic loads.

In Detroit, $SrBr_2$-based TES can surpass the Department of Energy (DOE)'s TES subprogram's target of $15/kWh thermal breakeven capital costs in cold climates in most homes (Figure 3). This DOE target can also be achieved with $SrBr_2$-based TES in all other cold-climate cities except Chicago. TES also has significant potential to be an effective peak demand reduction tool, particularly when operated with the main objective of maximizing peak demand shifting (i.e., as a demand response tool). When operating TES to maximize peak demand shifting, $SrBr_2$-based TES reduced between 12% and 27% peak load across all homes and reduced 395 MWh (11.6%) total peak load city-wide without raising total system costs. Therefore, mass adoption of TES can help utilities and balancing authorities reduce energy generating resources capacity deployment and contribute to improving systems flexibility and resource adequacy. Energy policies could incentivize TES adoption by households, e.g., through tax credits that are commonly used to encourage adoption of other technologies. TES could be compensated for peak reduction either directly from a utility or from a third-party aggregator, which is a supplemental revenue stream we do not capture in our analysis. However, given the rarity at which demand response events are called, demand response payments would likely be a small share of the overall TES cost savings from daily cycling.

Our work has several limitations that future work can address. First, to maintain computational tractability, we model heating demand and energy outputs from ASHP and TES energetically. Future research can combine detailed household designs with more detailed building integration modeling approaches, e.g., exergetic approaches,[10,34,39] to obtain more finely tuned valuations for high-value TES designs identified in our study. To what extent an exergetic approach would change the value of TES is unclear. Our ASHP COP estimates, for instance, are in general higher than those estimated in ResStock; higher COP estimates reduce the potential value of TES, so our results might undervalue the cost effectiveness of TES. Second, we focus on four salt hydrates as representative TES materials because they are widely studied for building heating and have experimentally reported operational data. Future studies could examine many other promising salt hydrates for RSH using our analytical framework and datasets.[54] Third, our study does not consider any TES

material-specific challenges, for example, stability to thermal cycling. Our modeling ignores cycling- and calendar-induced degradation of TES devices. Such degradation could reduce the long-term efficiency and/or power and energy capacities of a TES device, ultimately reducing its savings potential for households. Understanding the degradation of our analyzed TES devices is out of our scope. While all TES devices would likely experience degradation, cycling-induced degradation could be greater for a subset of our studied salt hydrates, e.g., $MgCl_2$, whose power and energy density characteristics lead them to cycle more to maximize household savings, as demonstrated in our results. Future work should quantify and capture the effects of degradation via long-term experiments and modeling in a similar line of work as a recent study of a $CaCl_2{\cdot}6H_2O$ graphite composite that demonstrated 90 cycles with minimal degradation.[55] Fourth, in our research, we calculate breakeven capital costs based on the savings for households from operation of TES devices. Future research can compare these breakeven capital costs with bottom-up cost estimates of salt hydrate TES devices integrated into households. Such bottom-up cost estimates would include costing of the salt hydrates, the reactor, and insulation, and depending upon the integration with the building's HVAC, it could also additionally include a heat exchanger, a humidifier, and a compressor. Integration costs may vary household to household, depending on the HVAC design. Non-salt hydrate costs may vary based on reactor volume, which in turn may vary between salt hydrates depending on the design priorities of the reactor. Finally, the Ragone plots for salts are more representative of ideal material performance dictated by intrinsic kinetics. Future studies could apply our techno-economic framework to Ragone plots that capture more real-world TES performance. However, given that our studied salt hydrate TES face challenging economics in the form of low breakeven capital costs (especially non-$SrBr_2$ hydrates), better capturing real-world TES design and operations (e.g., through inclusion of piping costs or Ragone plots for specific reactor designs) would not qualitatively affect our insights.

Despite these limitations and opportunities for future work, our research yields several important insights for salt hydrate TES research and development. Our findings emphasize the potential market of commercially produced salt hydrate TES to provide energy input for RSH demand and the potentially large role salt hydrate TES could play in decarbonizing the residential sector. We highlighted the attributes of salt hydrates that would make them more economically effective (high energy density, moderately high power density, and low humidification parasitic load), and the importance of TES sizing in driving optimal TES breakeven costs. Finally, we identified $SrBr_2$ as the most promising salt of the four we studied to be used as material in TES devices that can potentially bridge and exceed DOE's TES capital cost target in many cold-climate cities.

METHODS

Figure S1 illustrates how we model TES integration within RSH systems. Our building-level model allows for ASHP to serve hourly heating load as well as charge TES using electricity purchased from utilities. When ASHP runs, its heating fan operates to circulate air. The salt hydrate TES system is operated with a fan and humidifier. When TES charges, it uses air from ASHP. When salt hydrate TES discharges, a fan and humidifier run to maintain the home's humidification levels, and the TES uses recirculating air in the home. Our objective in this study is to provide a broad valuation of coupling salt hydrate TES systems with ASHPs for space heating within the US residential sector. We capture physical constraints on TES operations by integrating salt-hydrate-specific Ragone plots (see the supplemental information) within a techno-economic model of a RSH system (see the supplemental information). How a specific TES system would be integrated within each household's heating system would require detailed engineering analyses, which would require heating system schematics not available for a broad swath of US households. We therefore do not conduct specific integration analyses for each household. Rather, in our techno-economic model, we capture key factors that would affect the integration and performance of an open TES system, specifically balance-of-system losses and energy required for hydration during discharge of the TES device (see section TES materials and designs for more details).

Model for space heating with ASHP and TES

Our techno-economic model of RSH ("RSH model") is an optimization-based linear program that minimizes the total annual cost of purchasing electricity from a utility to meet RSH demand at the individual residential single family detached home ("residential home" or just "home") level. Decision variables in the RSH model are hourly operation of TES, hourly operation of ASHP, and hourly electricity purchases to power the ASHP. In the absence of TES, RSH is served by an ASHP with electric baseboard heating, electric furnace, or gas furnace as backup systems at low temperatures. When TES is coupled with the ASHP/electric baseboard heater system, energy output from ASHP can be used to charge (or store heat in) TES and/or to serve heating demand in any given hour. TES can use stored heat at a later time to provide heat to serve demand. Due to the characteristics of TES materials used in this study, TES cannot charge and discharge at the same time. Therefore, during the hours when TES is discharging to serve heating load, ASHP can assist in serving heating load only, and during the hours when TES is charging, ASHP runs to serve heating load and charge TES. Constraints require residential heating loads to be met, enforce salt-hydrate-specific relationships between state of charge (SOC) and maximum charge and discharge rates via piecewise linear approximations of the material-specific Ragone plots, and vary the ASHP's COP with ambient air temperatures. By running this model for RSH when TES is and is not coupled with an ASHP, we quantify cost savings and ASHP operational changes due to TES, as well as TES operations. For model details, please see the supplemental information.

To maintain computational tractability and a linear optimization, we model heating demand and energy outputs from ASHP and TES energetically (in units of kWh). The ASHP and TES devices used in this study are assumed to operate within the ranges of temperatures required for thermal comfort demands of our studied residential homes. Through our simplification of an energetic modeling approach, we can estimate the cost savings of diverse

TES materials across a large number of households and climate zones, providing broad insights into the value of TES. Future research can adopt more household-specific modeling approaches, e.g., exergetic approaches,[10,34,39] to obtain more finely tuned valuations for high-value TES designs identified in our study in smaller subsets of households.

To study the peak demand reduction, or demand response, potential of TES, we run a modified version of our RSH model that maximizes household peak load reduction instead of minimizing total cost (see the supplemental information).

TES materials and designs

For TES materials, we consider four types of salt hydrates: magnesium sulfate ($MgSO_4$), magnesium chloride ($MgCl_2$), potassium carbonate (K_2CO_3), and strontium bromide ($SrBr_2$) (Table 1). These salts are chosen as representative materials because they are widely studied for heating, have experimentally reported data for the reaction rates of hydration/dehydration of the salts, and have phase change dynamics vis-a-vis temperature and relative humidity amenable to RSH.[30] $MgSO_4$ represents a salt with high reaction enthalpy but relatively low specific power.[48] This is contrasted by K_2CO_3, which has low reaction enthalpy but high specific power.[50] $SrBr_2$ and $MgCl_2$ offer characteristics between these two extremes.[22,49,56] Finally, all four salts have temperature inputs and outputs during charging and discharging aligned with ASHP outlet temperatures and RSH needs, respectively.[30] As such, we ignore temperature in our RSH model and use instead an energy-based model, allowing us to quantify value across a large number of residential households.

Reaction rates influence power densities for discharging (or heat release) and charging (or heat storage) during hydration and dehydration reactions, respectively. This relationship is captured in Ragone plots, which we embed in our analysis using data and methods from Kinzer et al.[30] Thermogravimetric (TGA) measurements are typically operative under conditions where intrinsic, material-specific kinetics is the main limiting factor[57] and have been previously applied to salt hydrate TES.[30,57,58] Therefore, TGA measurements are agnostic to device design and represent the best-case power densities that can be accessed for a specific salt. While TGA discharge rates can be challenging to achieve in larger reactors, kinetic limitations become the primary constraining factor at high flow rates (around 0.25–0.5 m/s depending on salt and reactor design),[30,59] with additional optimization required to minimize additional parasitic losses including pumping costs to overcome air pressure drop. For instance, Kinzer et al.[30] and Aarts et al.[60] show the benefits of using larger millimeter sized and porous salt hydrate pellets to minimize pressure drop in a packed bed reactor. In this design, the hydration rate kinetics are limited by the ability of water vapor to diffuse into the pellets, so pellet size can be varied to achieve desired reaction rates. We use data from TGA measurements to obtain best-fit functions for the discharging and charging steps based on operating reaction temperatures and humidity.[30] In general, as the SOC approaches 0, reaction rates non-linearly decrease as there is less salt left to be hydrated.[50] During charging, the reactants and products flip, so reaction rates non-linearly decrease as the SOC approaches 1 (Figure S6). By controlling air temperature and relative humidity, it is possible to achieve similar reaction times for both recharging and discharging.[50] This allows us to simplify our model by assuming operating conditions that lead to a recharge curve that is a mirror image of the discharge curve with $sP_{discharging}(SOC = X) = sP_{charging}(SOC = 1 - X)$. Kinzer et al.[30] experimentally validate this Ragone framework using data for a packed bed reactor with $SrBr_2$ vermiculite composite particles. This approach allows assumed salt hydrate kinetics to compare performance across the different salt hydrates. Further explanation for the Ragone plots and specific traits of each salt are included in the supplemental information and Figure S6. Based on our operational conditions studied for salt hydrates, with relative humidity at most 30%, we ignore deliquescence in our salt hydrates.

For each salt hydrate, we assume integration would occur via an open TES system. When discharging, recirculating indoor air is humidified if needed and passed through the TES device. During discharging, we account for fan power consumption for recirculating air and account for parasitic losses due to humidification.[31] We estimate fan power consumption by generalizing results from NREL's ResStock analysis tool (see the supplemental information) and incorporate this fan power consumption in our RSH model (supplemental information). TES humidification needs will vary between households based on the household-specific space heating design, which is out of our analytical scope. Instead, we estimate parasitic losses from humidification for several alternative operational schemes. In each scheme, we estimate parasitic losses based on the heat of vaporization and the reaction enthalpy and vapor pressure requirements of each salt. Given the use of recirculating indoor air in our base case, we assume air flowing into the humidifier prior to the TES device is at 22°C and 20% relative humidity. In this base case, only $MgSO_4$ requires humidification of incoming air during discharging, resulting in a parasitic load of 39%. We test the sensitivity of our results to larger humidification needs that result in parasitic loads ranging from 44% to 70% (see section sensitivity analysis). Parasitic losses are incorporated in our model as a discharging efficiency penalty equal to one minus the parasitic load from humidification (parameter F_d in equation S6a). When charging, warm air from the ASHP is passed through the TES device. Power consumption during charging is accounted for in the ASHP operations [equation S4]). Finally, we account for other system losses through a round-trip efficiency penalty of 2%[61] but vary this parameter as well via sensitivity analysis.

We size each salt hydrate TES in three ways, reflecting different ways the mass of the salts for TES is determined when commercialized in the future: (1) variable TES sizing, (2) incremental (or step-wise) TES sizing, and (3) fixed TES sizing. Details of each sizing approach are in the supplemental information. Our main scenarios (discussed below) assume variable TES sizing, in which specific TES salt mass is sized to meet each home's peak heating load (kWh thermal), while other sizing methods are discussed in sensitivity analysis.

Residential data

We run our RSH model for 1 year (2018, to be consistent with the residential data, we use taken from Deetjen et al.[47]) for each of 400 representative residential homes in one cold-climate US

Table 2. Main scenarios for each of the 400 representative homes in each city of our study

Scenario	Coupled TES	TES material	TES sizing method
No TES (baseline)			
Scenario 1	no	–	–
TES sizes vary depending on buildings' peak loads			
Scenario 2 (*reference*)	yes	$SrBr_2$	variable
Scenario 3	yes	$MgCl_2$	variable
Scenario 4	yes	K_2CO_3	variable
Scenario 5	yes	$MgSO_4$	variable

city (Detroit, MI) as our main city of study, and for each of 400 representative single detached family homes in additional 11 US cities across different climates to capture the values of TES across different climate areas (see section scenarios design). This study design requires three key data inputs detailed in this section: hourly building-specific heating loads, hourly city-specific ASHP COPs, and hourly city-specific retail electricity rates.

We simulate the space heating load of these residential homes using NREL's ResStock analysis tool (version 2.2.5).[62] The ResStock analysis tool is a database of household characteristics for millions of US residential homes. Characteristics for each household are contained in an EnergyPlus file, allowing for bottom-up simulation of each household using EnergyPlus. From the ResStock database, we select 400 representative homes in each city to simulate in ResStock and then to run in our RSH model. A sample size of 400 homes captures most variability between single family detached homes in a given city, including 88%–96% of a city's annual heating demand,[47] allowing us to balance computational tractability with generalizability. Furthermore, ResStock was designed to run representative rather than all homes in a given region. To simulate hourly RSH load for each of our studied residential homes, we modify the building's heating source to electric baseboard heater (COP = 1), then simulate the building's operations in EnergyPlus for 2018. By using electric baseboard heat as the only heating device in a home, we capture the actual heating demand of that home given a COP of one, i.e., hourly energy input to the heater equals its hourly energy output to serve heating demand. Further details of how we use ResStock to simulate RSH loads by household are described in the supplemental information.

In the RSH model, we assume that each home already has an ASHP with a backup electric baseboard heater to serve heating demand. The electric baseboard heater provides heat at a COP of 1.0 during extreme cold (lower than $-17^{\circ}C$) when the ASHP's COP falls below 1.0 (see the supplemental information).

We estimate hourly ASHP COPs for each of our households using hourly city-specific weather data from 2018 and temperature-COP curves for a median cold-climate ASHP[63] (Figure S2). Hourly outdoor air temperature data for all homes in each city are obtained from automated surface/weather observing systems (ASOS/AWOS) at each city's major airport location,[64] which is the same weather data source as that used in ResStock.

To estimate cost savings from TES, we assume electricity to power the ASHP in our RSH model is purchased from a local distribution utility at a time-of-use retail rate that is the default/most popular rate of each state's major utility. We use time-of-use retail rate in our analysis to capture the ongoing trend of many utilities (such as DTE Energy, San Diego Gas and Electric, and Sacramento Municipal Utility District) increasingly implementing time-of-use rate as default retail rate for their customers, either as an alternative option to fixed retail rate or mandatory pricing rule to replace fixed retail rate. We obtain time-of-use rates from the most recent electric rate books of the utilities that are in charge of providing electricity to the buildings in the cities of our study. For Detroit, MI, which is within the service territory of DTE Energy, the fixed retail rate is 18.3¢/kWh and the time-of-use rate varies depending on the month and hour. Other cities' retail rates are shown in Table S6.

Scenarios design

To quantify the value of different TES designs coupled with ASHPs across climate zones, retail electricity rates, and households, we run five main scenarios for all representative homes in each city (Table 2). Scenario 1 meets space heating demand with only ASHP, which is powered by purchased electricity from grid at retail rate. Scenario 2, which is the reference scenario, couples $SrBr_2$-based TES using variable sizing with ASHP. Scenarios 3 through 5 facilitate similar comparisons with scenario 2 but using different salt hydrates as TES materials. Comparing these scenarios with scenario 1 captures the economic value of each TES design.

To quantify the value of TES in different climate areas, we run the above scenarios in 12 US cities: Atlanta, GA; Boston, MA; Detroit, MI; Chicago, IL; Dallas, TX; Denver, CO; Los Angeles, CA; Minneapolis, MN; New York, NY; Orlando, FL; Phoenix, AZ; and Seattle, WA.

Sensitivity analysis

We test the robustness of our results to alternative TES and ASHP configurations and operations (Table 3). Scenarios 6 through 13 facilitate similar comparisons with scenario 1 discussed above in section scenarios design using different salt hydrates but with incremental and fixed TES sizing. Scenario 16 assumes constant $SrBr_2$-based TES-specific power output of 100 W/kg, which is near the upper end of the range shown to be achievable with similar experimental prototypes.[24,53,65] Effective kinetics likely decrease from the TGA to the full reactor scale due in part to morphological changes in salt hydrate packing and temperature gradients, so this lower constant power output may be more representative of a real reactor.[30] Scenario 15 assumes that the TES-ASHP system is backed up by a gas furnace instead of an electric baseboard. Scenarios 16 through 19 consider alternative operational schemes with consequences on the parasitic load from humidification of air during TES discharging. Previous scenarios use humidification to fully provide the required humidity to the TES device when discharging, thereby not affecting inside humidity during TES discharging. Scenarios 16 and 17 increase the humidity of outdoor air assuming $0^{\circ}C$ air at 10% RH to that required for TES discharging. In these scenarios, parasitic loads for our salts range from 44% to 70%. In scenarios 18 and 19, we assume non-parasitic TES losses are 5% and 10%. All of these scenarios are run for Detroit, MI.

Table 3. Selected additional scenarios and sensitivity analysis of the study for each of the 400 representative homes in Detroit, MI

Scenario	Coupled TES	TES material	TES sizing method	City	TES design
Examining value of TES with incremental sizes					
Scenario 6	yes	$MgSO_4$	incremental	Detroit	reference
Scenario 7	yes	$MgCl_2$	incremental	Detroit	reference
Scenario 8	yes	K_2CO_3	incremental	Detroit	reference
Scenario 9	yes	$SrBr_2$	incremental	Detroit	reference
Examining value of TES with fixed sizes					
Scenario 10	yes	$MgSO_4$	fixed	Detroit	reference
Scenario 11	yes	$MgCl_2$	fixed	Detroit	reference
Scenario 12	yes	K_2CO_3	fixed	Detroit	reference
Scenario 13	yes	$SrBr_2$	fixed	Detroit	reference
Examining value of TES with different designs					
Scenario 14	yes	$SrBr_2$	variable	Detroit	constant rating (100 w/kg)
Scenario 15	yes	$SrBr_2$	variable	Detroit	gas furnace backup
Examining the consequences of high parasitic loads and other non-parasitic losses					
Scenarios 16 and 17	yes	all four salts	variable	Detroit	high parasitic load[a]
Scenarios 18 and 19	yes	$SrBr_2$	variable	Detroit	low round-trip efficiency[a]

[a]See the supplemental information for details.

RESOURCE AVAILABILITY

Lead contact

Questions or requests regarding this paper can be directed to the lead contact, An T. Pham (anph@umich.edu).

Materials availability

This research did not generate any new materials

Data and code availability

Data and model code are available at https://doi.org/10.5281/zenodo.15636164.

ACKNOWLEDGMENTS

We thank Dr. Parth Vaishnav from the University of Michigan's School for Environment and Sustainability (SEAS) for invaluable housing stock data guidance and suggestions, Dr. Claire McKenna from SEAS for expert insights into heat pump settings and operations, and Dr. Pamela Wildstein from SEAS for assistance with utilities' electric rate books. We also thank Dr. Steven Kiyabu from the University of Michigan's Department of Mechanical Engineering for initial assistance in choosing promising salts for this study. Funding for this research was provided by the Graham Sustainability Institute's Carbon Neutrality Acceleration Program (CNAP).

AUTHOR CONTRIBUTIONS

A.T.P.: conceptualization, techno-economic model development, model input preparation, results analysis & interpretation, writing – original draft, writing – review & editing, and visualization. B.K.: conceptualization, performing analyses to generate the Ragone plots as model input, identifying and selecting the salts investigated in this study, formulating and developing the Ragone framework for salt hydrates, and writing – review & editing. R.J.: performing ResStock simulation to obtain heating load profiles as model input. R.B.C.: conceptualization, identifying and selecting the salts investigated in this study, formulating and developing the Ragone framework for salt hydrates, results analysis & interpretation, writing – review & editing, supervision, and securing project funding. M.T.C.: conceptualization, model development, results analysis & interpretation, writing – review & editing, supervision, and securing project funding.

DECLARATION OF INTERESTS

The authors declare no competing interests.

SUPPLEMENTAL INFORMATION

Supplemental information can be found online at https://doi.org/10.1016/j.crsus.2025.100460.

Received: September 18, 2024
Revised: April 30, 2025
Accepted: July 7, 2025
Published: August 12, 2025

REFERENCES

1. IEA (2022). Buildings. Tech. Rep. (IEA). www.iea.org/reports/buildings
2. EIA (2022). Annual Energy Outlook 2022, Table 4. Residential sector key indicators and consumption. Tech. Rep. (EIA) www.eia.gov/outlooks/aeo/data/browser/#/?id=4-AEO2022&cases=ref2022&sourcekey=0
3. Lun, Y.V., and Tung, S.D. (2020). Heat Pumps for Sustainable Heating and Cooling (Springer). link.springer.com/book/10.1007/978-3-030-31387-6.
4. Langevin, J., Harris, C.B., and Reyna, J.L. (2019). Assessing the potential to reduce U.S. building CO_2 emissions 80% by 2050. Joule *3*, 2403–2424. https://doi.org/10.1016/j.joule.2019.07.013.
5. Fischer, D., Toral, T.R., Lindberg, K.B., Wille-Haussmann, B., and Madani, H. (2014). Investigation of thermal storage operation strategies with heat pumps in german multi family houses. Energy Procedia *58*, 137–144. https://doi.org/10.1016/j.egypro.2014.10.420.
6. Wu, W., and Skye, H.M. (2021). Residential net-zero energy buildings: Review and perspective. Renew. Sustain. Energy Rev. *142*, 110859. https://doi.org/10.1016/j.rser.2021.110859.
7. IEA (2022). Heat Pumps. Tech. Rep. (IEA). www.iea.org/reports/heat-pumps
8. Vaishnav, P., and Fatimah, A.M. (2020). The environmental consequences of electrifying space heating. Environ. Sci. Technol. *54*, 9814–9823. https://doi.org/10.1021/acs.est.0c02705.
9. Love, J., Smith, A.Z., Watson, S., Oikonomou, E., Summerfield, A., Gleeson, C., Biddulph, P., Chiu, L.F., Wingfield, J., Martin, C., et al. (2017). The

addition of heat pump electricity load profiles to GB electricity demand: Evidence from a heat pump field trial. Appl. Energy *204*, 332–342. https://doi.org/10.1016/j.apenergy.2017.07.026.

10. Arteconi, A., Hewitt, N.J., and Polonara, F. (2013). Domestic demand-side management (DSM): Role of heat pumps and thermal energy storage (TES) systems. Appl. Therm. Eng. *51*, 155–165. https://doi.org/10.1016/j.applthermaleng.2012.09.023.
11. Moreno, P., Solé, C., Castell, A., and Cabeza, L.F. (2014). The use of phase change materials in domestic heat pump and air-conditioning systems for short term storage: A review. Renew. Sustain. Energy Rev. *39*, 1–13. https://doi.org/10.1016/j.rser.2014.07.062.
12. Odukomaiya, A., Woods, J., James, N., Kaur, S., Gluesenkamp, K.R., Kumar, N., Mumme, S., Jackson, R., and Prasher, R. (2021). Addressing energy storage needs at lower cost via on-site thermal energy storage in buildings. Energy Environ. Sci. *14*, 5315–5329. https://doi.org/10.1039/D1EE01992A.
13. Renaldi, R., Kiprakis, A., and Friedrich, D. (2017). An optimisation framework for thermal energy storage integration in a residential heat pump heating system. Appl. Energy *186*, 520–529. https://doi.org/10.1016/j.apenergy.2016.02.067.
14. de Gracia, A., and Cabeza, L.F. (2017). Numerical simulation of a pcm packed bed system: A review. Renew. Sustain. Energy Rev. *69*, 1055–1063. https://doi.org/10.1016/j.rser.2016.09.092.
15. Li, Y., Huang, G., Xu, T., Liu, X., and Wu, H. (2018). Optimal design of PCM thermal storage tank and its application for winter available open-air swimming pool. Appl. Energy *209*, 224–235. https://doi.org/10.1016/j.apenergy.2017.10.095.
16. Osterman, E., and Stritih, U. (2021). Review on compression heat pump systems with thermal energy storage for heating and cooling of buildings. J. Energy Storage *39*, 102569. https://doi.org/10.1016/j.est.2021.102569.
17. Yu, M., Li, S., Zhang, X., and Zhao, Y. (2021). Techno-economic analysis of air source heat pump combined with latent thermal energy storage applied for space heating in China. Appl. Therm. Eng. *185*, 116434. https://doi.org/10.1016/j.applthermaleng.2020.116434.
18. Zhao, B.C., and Wang, R.Z. (2019). Perspectives for short-term thermal energy storage using salt hydrates for building heating. Energy *189*, 116139. https://doi.org/10.1016/j.energy.2019.116139.
19. Du, R., Wu, M., Wang, S., Wu, S., Wang, R., and Li, T. (2022). Experimental investigation on high energy-density and power-density hydrated salt-based thermal energy storage. Appl. Energy *325*, 119870. https://doi.org/10.1016/j.apenergy.2022.119870.
20. Li, Y., Li, C., Lin, N., Xie, B., Zhang, D., and Chen, J. (2021). Review on tailored phase change behavior of hydrated salt as phase change materials for energy storage. Mater. Today Energy *22*, 100866. https://doi.org/10.1016/j.mtener.2021.100866.
21. Oró, E., de Gracia, A., Castell, A., Farid, M.M., and Cabeza, L.F. (2012). Review on phase change materials (PCMs) for cold thermal energy storage applications. Appl. Energy *99*, 513–533. https://doi.org/10.1016/j.apenergy.2012.03.058.
22. Cammarata, A., Verda, V., Sciacovelli, A., and Ding, Y. (2018). Hybrid strontium bromide-natural graphite composites for low to medium temperature thermochemical energy storage: Formulation, fabrication and performance investigation. Energy Convers. Manag. *166*, 233–240. https://doi.org/10.1016/j.enconman.2018.04.031.
23. Donkers, P.A.J., Sögütoglu, L.C., Huinink, H.P., Fischer, H.R., and Adan, O.C.G. (2017). A review of salt hydrates for seasonal heat storage in domestic applications. Appl. Energy *199*, 45–68. https://doi.org/10.1016/j.apenergy.2017.04.080.
24. Michel, B., Mazet, N., Mauran, S., Stitou, D., and Xu, J. (2012). Thermochemical process for seasonal storage of solar energy: Characterization and modeling of a high density reactive bed. Energy *47*, 553–563. https://doi.org/10.1016/J.ENERGY.2012.09.029.
25. Kenisarin, M., and Mahkamov, K. (2016). Salt hydrates as latent heat storage materials:thermophysical properties and costs. Sol. Energy Mater. Sol. Cells *145*, 255–286. https://doi.org/10.1016/j.solmat.2015.10.029.
26. Wang, Y., Yu, K., and Ling, X. (2019). Experimental and modeling study on thermal performance of hydrated salt latent heat thermal energy storage system. Energy Convers. Manag. *198*, 111796. https://doi.org/10.1016/j.enconman.2019.111796.
27. Kumar, N., Ness, R.V., Chavez, J., Reynaldo, B., D., Muley, A., and Stoia, M. (2021). Experimental analysis of salt hydrate latent heat thermal energy storage system with porous aluminum fabric and salt hydrate as phase change material with enhanced stability and supercooling. J. Energy Resour. Technol. *143*, 042001. https://doi.org/10.1115/1.4048122.
28. Wang, Y., Yu, K., and Ling, X. (2020). Experimental study on thermal performance of a mobilized thermal energy storage system: A case study of hydrated salt latent heat storage. Energy Build. *210*, 109744. https://doi.org/10.1016/j.enbuild.2019.109744.
29. Pardiñas, Á.Á., Alonso, M.J., Diz, R., Kvalsvik, K.H., and Fernández-Seara, J. (2017). State-of-the-art for the use of phase-change materials in tanks coupled with heat pumps. Energy Build. *140*, 28–41. https://doi.org/10.1016/j.enbuild.2017.01.061.
30. Kinzer, B., Ghosh, D.P., Crowley, D., Jatkar, A., and Bala Chandran, R.B. (2025). Impact of scaling and design on salt hydrate thermochemical energy storage performance. Appl. Therm. Eng. *272*, 126160. https://doi.org/10.1016/j.applthermaleng.2025.126160.
31. N'Tsoukpoe, K.E., and Kuznik, F. (2021). A reality check on long-term thermochemical heat storage for household applications. Renew. Sustain. Energy Rev. *139*, 110683. https://doi.org/10.1016/j.rser.2020.110683.
32. Wang, Z., Wang, F., Ma, Z., Lin, W., and Ren, H. (2019). Investigation on the feasibility and performance of transcritical co_2 heat pump integrated with thermal energy storage for space heating. Renew. Energy *134*, 496–508. https://doi.org/10.1016/j.renene.2018.11.035.
33. Teamah, H.M., and Lightstone, M.F. (2019). Numerical study of the electrical load shift capability of a ground source heat pump system with phase change thermal storage. Energy Build. *199*, 235–246. https://doi.org/10.1016/j.enbuild.2019.06.056.
34. Farah, S., Liu, M., and Saman, W. (2019). Numerical investigation of phase change material thermal storage for space cooling. Appl. Energy *239*, 526–535. https://doi.org/10.1016/j.apenergy.2019.01.197.
35. Wu, P., Wang, Z., Li, X., Xu, Z., Yang, Y., and Yang, Q. (2020). Energy-saving analysis of air source heat pump integrated with a water storage tank for heating applications. Build. Environ. *180*, 107029. https://doi.org/10.1016/j.buildenv.2020.107029.
36. Le, K.X., Huang, M.J., Shah, N.N., Wilson, C., Artain, P.M., Byrne, R., and Hewitt, N.J. (2019). Techno-economic assessment of cascade air-to-water heat pump retrofitted into residential buildings using experimentally validated simulations. Appl. Energy *250*, 633–652. https://doi.org/10.1016/j.apenergy.2019.05.041.
37. Masip, X., Cazorla-Marín, A., Montagud-Montalvá, C., Marchante, J., Barceló, F., and Corberán, J.M. (2019). Energy and techno-economic assessment of the effect of the coupling between an air source heat pump and the storage tank for sanitary hot water production. Appl. Therm. Eng. *159*, 113853. https://doi.org/10.1016/j.applthermaleng.2019.113853.
38. Zhu, N., Hu, P., Lei, Y., Jiang, Z., and Lei, F. (2015). Numerical study on ground source heat pump integrated with phase change material cooling storage system in office building. Appl. Therm. Eng. *87*, 615–623. https://doi.org/10.1016/j.applthermaleng.2015.05.056.
39. D'Ettorre, F., De Rosa, M., Conti, P., Testi, D., and Finn, D. (2019). Mapping the energy flexibility potential of single buildings equipped with optimally-controlled heat pump, gas boilers and thermal storage. Sustain. Cities Soc. *50*, 101689. https://doi.org/10.1016/j.scs.2019.101689.

40. Zeng, Y., Clark, R.J., Galazutdinova, Y., Odukomaiya, A., Al-Hallaj, S., Farid, M., Kaur, S., and Woods, J. (2024). Open-cycle thermochemical energy storage for building space heating: Practical system configurations and effective energy density. Appl. Energy *376*, 124218. https://doi.org/10.1016/j.apenergy.2024.124218.

41. Christen, T., and Carlen, M.W. (2000). Theory of ragone plots. J. Power Sources *91*, 210–216. https://doi.org/10.1016/S0378-7753(00)00474-2.

42. Woods, J., Mahvi, A., Goyal, A., Kozubal, E., Odukomaiya, A., and Jackson, R. (2021). Rate capability and ragone plots for phase change thermal energy storage. Nat. Energy *6*, 295–302. https://doi.org/10.1038/s41560-021-00778-w.

43. James, N., Mahvi, A., and Woods, J. (2022). Optimizing phase change composite thermal energy storage using the thermal ragone framework. J. Energy Storage *56*, 105875. https://doi.org/10.1016/J.EST.2022.105875.

44. Yazawa, K., Shamberger, P.J., and Fisher, T.S. (2019). Ragone relations for thermal energy storage technologies. Front. Mech. Eng. *5*. https://doi.org/10.3389/fmech.2019.00029.

45. Teichert, O., Link, S., Schneider, J., Wolff, S., and Lienkamp, M. (2023). Techno-economic cell selection for battery-electric long-haul trucks. eTransportation *16*, 100225. https://doi.org/10.1016/j.etran.2022.100225.

46. Vykhodtsev, A.V., Jang, D., Wang, Q., Rosehart, W., and Zareipour, H. (2022). A review of modelling approaches to characterize lithium-ion battery energy storage systems in techno-economic analyses of power systems. Renew. Sustain. Energy Rev. *166*, 112584. https://doi.org/10.1016/j.rser.2022.112584.

47. Deetjen, T.A., Walsh, L., and Vaishnav, P. (2021). US residential heat pumps: the private economic potential and its emissions, health, and grid impacts. Environ. Res. Lett. *16*, 084024. https://doi.org/10.1088/1748-9326/ac10dc.

48. Linnow, K., Niermann, M., Bonatz, D., Posern, K., and Steiger, M. (2014). Experimental studies of the mechanism and kinetics of hydration reactions. Energy Procedia *48*, 394–404. https://doi.org/10.1016/j.egypro.2014.02.046.

49. Hawwash, A.A., Hassan, H., and feky, K.E. (2020). Impact of reactor design on the thermal energy storage of thermochemical materials. Appl. Therm. Eng. *168*, 114776. https://doi.org/10.1016/J.APPLTHERMALENG.2019.114776.

50. Gaeini, M., Shaik, S.A., and Rindt, C.C.M. (2019). Characterization of potassium carbonate salt hydrate for thermochemical energy storage in buildings. Energy Build. *196*, 178–193. https://doi.org/10.1016/J.ENBUILD.2019.05.029.

51. DOE (2022). Buildings energy efficiency frontiers & innovation technologies (benefit) – 2022/23. Tech. Rep. (DOE).

52. DOE. (2017). 2017 Building America climate-specific guidance. www.energy.gov/eere/buildings/climate-zones.

53. Zhang, Y., Dong, H., Wang, R., and Feng, P. (2020). Air humidity assisted sorption thermal battery governed by reaction wave model. Energy Storage Mater. *27*, 9–16. https://doi.org/10.1016/J.ENSM.2020.01.012.

54. Clark, R.J., Gholamibozanjani, G., Woods, J., Kaur, S., Odukomaiya, A., Al-Hallaj, S., and Farid, M. (2022). Experimental screening of salt hydrates for thermochemical energy storage for building heating application. J. Energy Storage *51*, 104415. https://doi.org/10.1016/j.est.2022.104415.

55. Galazutdinova, Y., Clark, R.J., Al-Hallaj, S., Kaur, S., and Farid, M. (2024). New thermochemical salt hydrate system for energy storage in buildings. Energies *17*, 5228. https://doi.org/10.3390/en17205228.

56. Fisher, R., Ding, Y., and Sciacovelli, A. (2021). Hydration kinetics of K_2CO_3, $MgCl_2$ and vermiculite-based composites in view of low-temperature thermochemical energy storage. J. Energy Storage *38*, 102561. https://doi.org/10.1016/j.est.2021.102561.

57. Mahmoudi, A., Donkers, P.A., Walayat, K., Peters, B., and Shahi, M. (2021). A thorough investigation of thermochemical heat storage system from particle to bed scale. Chem. Eng. Sci. *246*, 116877. https://doi.org/10.1016/J.CES.2021.116877.

58. Ye, Z., Liu, H., Wang, W., Liu, H., Lv, J., and Yang, F. (2022). Reaction/sorption kinetics of salt hydrates for thermal energy storage. J. Energy Storage *56*, 106122, www.sciencedirect.com/science/article/pii/S2352152X22021107. https://doi.org/10.1016/j.est.2022.106122.

59. de Jong, S. (2022). Modelling salt hydration in packed beds for thermochemical heat storage purposes. Master's thesis (Eindhoven University of Technology).

60. Aarts, J., de Jong, S., Cotti, M., Donkers, P., Fischer, H., Adan, O., and Huinink, H. (2022). Diffusion limited hydration kinetics of millimeter sized salt hydrate particles for thermochemical heat storage. J. Energy Storage *47*, 103554. https://doi.org/10.1016/j.est.2021.103554.

61. De Boer, R., Smeding, S., Zondag, H., and Krol, G. (2014). Development of a prototype system for seasonal solar heat storage using an open sorption process. In Conference: Advances in Thermal Energy Storage.

62. Wilson, E.J. (2017). Resstock - targeting energy and cost savings for u.s. homes (NREL). www.osti.gov/biblio/1398250.

63. Waite, M., and Modi, V. (2020). Electricity load implications of space heating decarbonization pathways. Joule *4*, 376–394. https://doi.org/10.1016/j.joule.2019.11.011.

64. IEM (2025). Iowa Environmental Mesonet. mesonet.agron.iastate.edu/request/download.phtml.

65. Yan, T., Li, T., Xu, J., Chao, J., Wang, R., Aristov, Y.I., Gordeeva, L.G., Dutta, P., and Murthy, S.S. (2021). Ultrahigh-energy-density sorption thermal battery enabled by graphene aerogel-based composite sorbents for thermal energy harvesting from air. ACS Energy Lett. *6*, 1795–1802. https://doi.org/10.1021/acsenergylett.1c00284.